Stepwise Subunit Interaction Changes by Mono- and Bisphosphorylation of Cardiac Troponin I†

Silke U. Reiffert, Kornelia Jaquet, Ludwig M. G. Heilmeyer, Jr., and Friedrich W. Herberg*

Ruhr-Universität Bochum, Institut für Physiologische Chemie, Abt. Biochemie Supramolekularer Systeme, Universitätsstrasse 150, D-44801 Bochum, Germany

Received February 3, 1998; Revised Manuscript Received July 6, 1998

ABSTRACT: Four phosphorylation degrees of cardiac troponin I (cTnI) have been characterized, namely, a dephospho, a bisphospho, and two monophospho states. Here we describe for the first time a role of the monophosphorylated forms. We have investigated the interaction between the cardiac troponin subunits dependent on the phosphorylation state of cTnI by surface plasmon resonance (SPR) spectroscopy. The monophosphorylated forms were generated by mutating each of the two serine residues, located in human cTnI at positions 22 and 23, to alanine. Association and dissociation rate constants of binary (cTnI−cTnT and cTnI−cTnC) and ternary (cTnI/cTnC complex−cTnT) complexes were determined. Mono- and consecutive bisphosphorylation of cTnI gradually reduces the affinity to cTnC and cTnT by lowering the association rate constants; the dissociation rate constants remain unchanged. Phosphorylation also affects formation of the ternary complexes; however, in this instance, association rate constants are constant, and dissociation rate constants are enhanced. A model of cardiac troponin is presented describing an induction of distinct conformational changes by mono- and bisphosphorylation of cTnI.

Cardiac troponin (cTn),[1] a major regulatory protein of thin filaments, is composed of three subunits: cTnT (tropomyosin binding subunit), cTnI (inhibitory subunit), and cTnC (calcium binding subunit). Upon binding of calcium to cTnC, conformational changes occur within the proteins of the thin filament finally releasing the actomyosin ATPase inhibition. A key event seems to be a change in the interaction between cTnI and cTnC as well as between actin and cTnI [for review, see (*1*, *2*)].

In heart, the regulation of contraction by calcium is modulated additionally by phosphorylation and dephosphorylation. β-Adrenergic stimulation results in an increase of the cTnI phosphorylation degree up to 2 mol of phosphate/mol of protein; incorporation of about 1 mol of phosphate/mol of cTnI correlates with an increase in the force of contraction (*3*−*5*).

The heart-specific N-terminus of cTnI contains two adjacent serine residues that can be phosphorylated by the cAMP-dependent protein kinase (PKA) [positions 22 and 23 of the human cTnI sequence (*6*−*9*)]. Kinetic studies have shown that serine 23 is phosphorylated about 12-fold faster than serine 22 (*10*). Similarly, protein phosphatase 2A (PP2A) catalyzes hydrolysis of phosphoserine 23 ca. 2-fold faster than that of phosphoserine 22. By the combined action of PKA and PP2A, a cycling process is generated which produces one dephospho-, two mono-, and one bisphosphorylated cTnI forms (*11*). All these forms are found in cTnI isolated from heart (*6*, *7*, *12*).

Two sets of experiments, on the one hand with skinned fibers (*13*−*15*) and on the other hand with reconstituted thin filaments to which a calcium-dependent binding of myosin subfragment S1 is determined (*16*), demonstrate that bisphosphorylation of cTnI decreases the calcium sensitivity in both these systems. What remains unclear is the function of the monophosphorylated forms. Monophosphorylation does not seem to influence the calcium-induced contraction of skinned fibers (*13*).

^{31}P NMR spectra, employing the cTn holocomplex, show that the two adjacent phosphoserine residues present in bisphosphorylated cTnI are in a chemical environment which differs from that of each phosphoserine, when present in each of the two monophosphorylated forms. It suggests that there are structural differences between all cTnI forms mentioned (*17*). Therefore, we investigated the interaction between the cTn subunits by reconstituting a cTn holocomplex and a cTn/Tm (tropomyosin) complex on sensor chips to follow complex formation and dissociation by surface plasmon resonance spectroscopy (SPR). For that purpose, all cTnI subunit forms, especially the monophospho forms, had to be isolated preparatively. The monophospho forms were obtained by cloning the human cTnI cDNA and subsequently

† Supported by grants from the Deutsche Forschungsgemeinschaft (SFB394), the H. und G. Fischer Stiftung, and the Fonds der Chemie.

* To whom correspondence should be addressed. Telephone: (+49) (0)234 700 4934. FAX: (+49) (0)234 709 4193. E-mail: friedrich.w.herberg@ruhr-uni-bochum.de.

[1] Abbreviations: BSA, bovine serum albumin; cAMP, adenosine 3′,5′-cyclic monophosphate; cTn, cardiac troponin; cTnI, cTnT, cTnC, cardiac troponin I, T, C; sTnI, sTnT, sTnC, skeletal troponin I, T, C; cTnI-WT, recombinant wild-type cardiac troponin I; DTT, dithiothreitol; EDC, *N*-ethyl-*N*′-(3-diethylaminopropyl)carbodiimide; EGTA, ethylene glycol bis(β-aminoethyl ether)-*N*,*N*,*N*′,*N*′-tetraacetic acid; FITC, fluorescein-5-isothiocyanate; HABA, 2-(4′-hydroxyazobenzene)benzoic acid; IEF, isoelectric focusing; MOPS, 3-(*N*-morpholino)propanesulfonic acid; NHS, *N*-hydroxysuccinimido; PCR, polymerase chain reaction; PKA, cAMP-dependent protein kinase; PMSF, phenylmethylsulfonyl fluoride; PP2A, protein phosphatase 2A; RU, response units (1000 RU = 1 ng of protein/mm^2); R_{eq}, equilibrium response level; SDS, sodium dodecyl sulfate; SPR, surface plasmon resonance; Tm, tropomyosin.

S0006-2960(98)00280-3 CCC: $15.00
Published on Web 09/05/1998

by creating mutants in which either serine 22 or serine 23 was replaced by alanine. Phosphorylation by PKA produces the monophospho forms needed. Additionally, all phosphorylation states of cTnI were mimicked by replacing each serine with aspartate.

It will be shown for the first time that phosphorylation of each of the serines, 22 or 23, of cTnI affects the interaction with cTnC and cTnT. Bisphosphorylation exerts a stronger effect. Thus, each phosphorylation step, mono- and consecutive bisphosphorylation, changes the conformation of cTnI itself and of the holocomplex stepwise.

MATERIALS AND METHODS

Construction of Plasmids Expressing cTnI, Its Mutants, and cTnC. The human cDNA of cardiac troponin I (cTnI) was obtained by polymerase chain reaction (PCR) using the λ-DNA of a human cardiac cDNA library in λ-ZAPII-vector (Stratagene) as template. For amplification by PCR, the following oligonucleotides were employed as the sense and antisense primer: (1) 5′-GAATTCATATGGGAGCAGCGATGCG-3′ and (2) 5′-AAGCTTGGATCCAGGAAGGCTCAGCTCTC-3′, which contained the *Nde*I and *Bam*HI restriction sites for subcloning into the *Nde*I−*Bam*HI site of pET-3c (Stratagene), a T7 promoter based vector. To overexpress cTnI, the sequences of the second and fourth codons were changed (Ala2: GCG→GCC and Gly4: GGG→GGT) according to (*18*).

The cTnI-S22A and cTnI-S23A mutants were created with the chameleon mutagenesis method of Stratagene. The following oligonucleotide was employed to generate cTnI-S22A: 5′-GCGGTAGTTGGAGGCGCGGCGTCTGATTG-3′, and 5′-AGCGCGGATGTTGGCGGAGCGGCGTCTGA-3′ to generate cTnI-S23A.

To obtain cTnI where a single or both serines are replaced by aspartate, the following oligonucleotides were used to create the mutation via inside-out PCR: (1) 5′-GCGGCGTCTGATTGGGGCTGGTGCAG-3′ for the cTnI-S22D mutant, where serine 22 is replaced by aspartate; (2) 5′-GACAACTACCGCGCTTATGCCACGGAGCC-3′ for the cTnI-S23D mutant, where serine 23 is replaced by aspartate. By using both oligonucleotides, we obtained the cTnI-S22D-S23D double mutant.

The cDNA of human cTnC was obtained from the clone (*19*). Prior to subcloning into a pET-3c vector, a PCR amplification was performed using primers identical to those of (*18*).

Expression and Purification of Recombinant Proteins. cTnI-WT, cTnI-S22A, cTnI-S23A, cTnI-S22D, cTnI-S23D, cTnI-S22D-S23D, and human cTnC were expressed in *E. coli* BL21(DE3). Cells were grown in NZCYM medium with 200 μg/mL ampicillin at 37 °C until $OD_{600} = 0.6$; then cells were induced with 0.4 mM IPTG and grown for an additional 4 h period. The cell pellets from a 1 L culture of any cTnI clone were lysed in 50 mM potassium phosphate, 8 mM EDTA, 2 mM PMSF, and 2 mM DTT, pH 7.0, using a French Press (Aminco). The protein, present in inclusion bodies, was dissolved by adding 8 M urea (ultrapure; Gibco) to a volume of approximately 5 mL of buffer per 250 mL of original cell culture. After incubation for 1.5 h at room temperature and centrifugation at 48000*g* for 30 min, the supernatant was diluted to obtain final concentrations of 50 mM potassium phosphate, 6 M urea, 4 mM EDTA, 1 mM PMSF, and 1 mM DTT, pH 7.0 (buffer A). Then 30 mL of CM-Sepharose fast flow (Pharmacia) was equilibrated in buffer A and incubated with the supernatant of 1 L of original culture. After washing the resin with buffer A, cTnI was eluted by 0.6 M NaCl in 30 mL of buffer A. For further purification, the protein was applied onto a cTnC-affinity column [column preparation according to (*13*)] in 50 mM Tris, 0.5 M NaCl, 3 M urea, 2 mM $CaCl_2$, and 1 mM DTT, pH 7.5 (buffer B), washed with buffer B, and eluted with 6 M urea and 5 mM EDTA in 50 mM Tris, 0.5 M NaCl, and 2 mM DTT, pH 7.5. The protein was then dialyzed in 20 mM MOPS, 0.3 M KCl, 5 mM $MgCl_2$, and 2 mM DTT, pH 7.0 (buffer C), and stored on ice. A yield of 25 mg of pure cTnI per liter of culture was achieved.

cTnC was overexpressed in *E. coli* and purified as described by (*20*), giving a yield of 100 mg of cTnC per liter of culture.

Phosphorylation of cTnI-WT, cTnI-S23A, and cTnI-S22A. A 200 nmol sample of each protein, cTnI-WT, cTnI-S23A, and cTnI-S22A was phosphorylated with 300, 100, and 50 milliunits of recombinant catalytic subunit of PKA, respectively, for 1 h at 30 °C in buffer C containing 1 mM ATP. The phosphate content was determined by incorporation of [^{32}P]phosphate, and phospho forms were separated by IEF.

Formation of the cTnI−cTnC and cTn Complexes. cTnT was specifically dephosphorylated within the bovine cTn complex according to (*21*) prior to isolation from the cTn holocomplex in 6 M urea according to (*22*). The cTnI and cTnC subunits were overexpressed in *E. coli* as described above.

The binary complexes were formed by combining cTnI/cTnC and cTnI/cTnT in a molar ratio of 1:1 in 50 mM Tris, 6 M urea, 0.5 M NaCl, 5 mM $CaCl_2$, and 5 mM DTT, pH 7.5. The ternary complexes were formed accordingly in the same buffer by combining cTnI, cTnC, and cTnT in equal molar ratios. After incubation for 1 h at room temperature, at first urea was removed stepwise by dialysis at 4 °C from 6 to 5, 4, 3, 2, and finally to 1 M in buffer C with 1 M KCl and 0.1 mM $CaCl_2$, and, second, KCl was reduced stepwise from 1 to 0.75, 0.5, and finally to 0.3 M. Dialysis was performed for at least 3 h per step in 50 times the volume.

To remove any excess of cTn subunit and to verify complex formation of the ternary and binary complexes, Sephadex G-100 (Pharmacia, 2.5 × 100 cm) and Superdex G-75 (Pharmacia, 2.5 × 100 cm) gel filtration column were used, respectively. Gel filtration was performed in 10 mM MOPS, 0.5 M KCl, 1.5 mM $CaCl_2$, and 1 mM DTT, pH 7.0.

Fluorescence Labeling. cTnC was labeled with fluorescein 5-isothiocyanate (FITC, Molecular Probes) at room temperature in 50 mM $NaHCO_3$, pH 8.5, and a 10-fold molar excess of FITC. The reaction was stopped after 30 min by passing the reaction mixture through a prepacked Sephadex G-25 column (NAP10, Pharmacia) equilibrated with 20 mM MOPS, 0.5 M KCl, 5 mM $MgCl_2$, 0.1 mM $CaCl_2$, and 2 mM DTT, pH 8.0 (buffer D).

Analytical Gel Filtration. Analytical gel filtration was carried out using a Sephadex 200 PC 3.2/30 column (Pharmacia) with a flow rate of 80 μL/min at room

temperature in buffer D on the Smart-System (Pharmacia) according to (*23*).

For K_D determinations, a stock solution of 12 μM holocomplex was prepared by combining cTnT (dephosphorylated, bovine), cTnI, and cTnC labeled with FITC in a molar ratio of 1:1:1. Dilutions of this stock solution were incubated at 4 °C overnight before applying 50 μL on the column. cTnC-containing complexes were detected by monitoring fluorescence at 520 nm. Calibration was performed with protein standards of Pharmacia (low). The void volume (υ_0) was determined with blue dextran. FITC-labeled protein was detected with a fluorescence detector (GAT, Bremen) at an excitation wavelength of 495 nm and an emission wavelength of 520 nm. The free subunits or the cTnI/cTnC complex can be readily distinguished from the holocomplex via their retention times. The percentage of holocomplex at various protein concentrations was calculated by integrating the peak areas after base line correction. No quenching of the fluorescence signal due to the formation of the holocomplex with cTnC−FITC could be detected.

Biotin Labeling. cTnC, cTnT, and Tm were biotinylated in 50 mM $NaHCO_3$, pH 8.5, in 20 mM MOPS, 0.3 M KCl, 5 mM $MgCl_2$, and 2 mM DTT, pH 8.0, and in buffer C with 0.15 M KCl, respectively, with a 3-fold molar excess of NHS−Biotin (Pierce) at 4 °C. Coupling of biotin to lysine residues was stopped after 2 h by passing the reaction mixture through a prepacked Sephadex G-25 column (PD-10, Pharmacia) equilibrated in 20 mM MOPS, 0.3 M KCl, and 1 mM DTT, pH 7.0. The biotinylation degree was determined by HABA−Avidin Reagent (Sigma).

Surface Plasmon Resonance (SPR). Studies on the interaction between the cTn subunits were performed by SPR spectroscopy using a Biacore 2000 instrument. Here one binding partner, referred to as the ligand, is immobilized on a sensor chip, and the interaction with an interactant in free solution, the analyte, is detected. Changes in the mass concentration are proportional to changes in the refractive index on the sensor surface, resulting in changes in the SPR signal [for review of the technique, see (*24*)]. To summarize the phenomenon, light reflected at an interface between media of two refractive indices separated by a thin film of conducting material will resonate (surface plasmon resonance) at a specific angle and result in a reduction in intensity of the reflected light at that angle. The angle is very sensitive to refractive index changes in the less dense medium on the opposite side of the interface from the incident and reflected light. In general, the refractive index change for a given change of mass concentration at the surface layer is practically the same for all proteins and peptides (*25*). The change in the resonance angle is expressed in response units (RU). A response (i.e., a change in the resonance signal) of 1000 RU corresponds to a change in the surface concentration on the sensor chip of about 1 ng of protein/mm^2 (*25*). cTnC and cTnT, derivatized with biotin, were captured by immobilized streptavidin (SA5-chip) to the chip surface by injecting 0.01 mg/mL of the biotinylated proteins and adjusting the immobilization level to 1000 RU and 500 RU for cTnC and cTnT, respectively. To determine unspecific binding, runs were performed with identical samples and solutions using a streptavidin surface without captured protein. To study the interaction between the cTn subunits, buffer D and a flow rate of 10 μL/min were employed. For Ca^{2+}-free measurements, 2 mM EGTA was added to buffer D instead of $CaCl_2$. The cTnC complexes formed were designated as described by (*26*). Both the association and dissociation phases were measured in the same buffer. Regeneration of the surface was achieved by injecting 20 μL of 3 M urea, 1 M KCl, 10 mM EDTA, and 2 mM EGTA.

Surface activity was calculated using the equation: $S = MW_L R_A / MW_A R_L$ where S is the stoichiometry, subscript L defines ligand (immobilized protein), subscript AL defines analyte (injected protein), R represents response in RU's, and MW is the molecular weight of the ligand or analyte.

Constants for the rates of association and dissociation of free analyte to the bound ligand were calculated from the changes in response by nonlinear regression using the Biaevalution 2.1 software. Control experiments were performed to detect mass-transfer limited interactions affecting the kinetics (*27*). Therefore, first, sensor chips were produced with varied ligand density on the surface, and, second, the flow rate was changed to overcome potential mass-transfer limitations. However, no differences in the rate constants obtained were detected (data not shown).

The association and the dissociation rate for binary complex formation is described by

$$A + B \underset{k_d}{\overset{k_a}{\rightleftharpoons}} AB \tag{1}$$

where k_a and k_d are the rate constants for the formation of the complex. The association rate is

$$d[AB]/dt = k_a[A][B] \tag{2}$$

and the dissociation rate is

$$-d[AB]/dt = k_d[AB] \tag{3}$$

At equilibrium, association and dissociation equals

$$K_D = [A][B]/[AB] = k_d/k_a \tag{4}$$

or

$$K_A = [AB]/[A][B] = k_a/k_d \tag{5}$$

where K_D and K_A are the equilibrium dissociation and equilibrium association binding constants, respectively.

If mass transfer is much faster than interaction-controlled association, the analyte at the surface is maintained at the same concentration as in the bulk phase, and the rate equation can be written as

$$d[AB]/dt = k_a[A][B] - k_d[AB] \tag{6}$$

The concentration of unoccupied ligand, [B], is the difference between the total amount of ligand on the surface, $[B]_0$, and the amount of complex, [AB]:

$$[B] = [B]_0 - [AB] \tag{7}$$

Substitution of 6 yields

$$d[AB]/dt = k_a[A]([B]_0 - [AB]) - k_d[AB] \tag{8}$$

If the total amount of ligand, $[B]_0$, is expressed in terms of the maximum analyte binding capacity of the surface, all

concentration terms can then be expressed as SPR response in RU, eliminating the need to convert from mass to molar concentration:

$$dR/dt = k_a C(R_{max} - R) - k_d R \quad (9)$$

where dR/dt is the rate of change of the SPR signal, C the concentration of the injected analyte, R_{max} the maximum analyte binding capacity of the sensor surface in RU, and R the SPR signal at time t.

The equation can be rearranged to give

$$dR/dt = k_a C R_{max} - (k_a C + k_d)R \quad (10)$$

Equation 10 can be solved analytically if C is assumed to be constant (which is a valid approximation using dispersion-free injection of the sample). Separating variables and integrating yield

$$R = k_a C R_{max}/(k_a C + k_d)[1 - e^{-(k_a + k_d)t}] \quad (11)$$

This equation describes the response at any time during association and can be used for nonlinear regression analysis of single curves.

Following eq 3 and the considerations leading to eq 9, the dissociation phase can be described as

$$dR/dt = -k_d R \quad (12)$$

assuming that the reassociation of released analyte (rebinding) is negligible. Dissociation kinetics were checked for rebinding effects by co-injecting nonbiotinylated ligand in the same concentrations as the immobilized ligand during the dissociation phase.

Separating variables and integrating yield

$$R_t = R_0 e^{-k_d(t - t_0)} \quad (13)$$

where R_t is the response at time t and R_0 the time at an arbitrary starting point t_0.

Statistical Analysis. Statistical analysis of the data was performed using the software Graphpad Statmat and Graphpad Prism. Each set of binding isotherms was analyzed in the association and dissociation phases separately. Standard deviations were calculated using unpaired *t*-test analysis (one way anova) assuming parametric conditions. The Newman−Keuls post test was selected to compare pairs of group means. Values were defined as statistically significantly different with p-values < 0.05.

RESULTS

Specifically monophosphorylated states of cTnI carrying phosphate either at serine 22 or at serine 23 cannot be obtained preparatively employing native cTnI. Phosphorylation by PKA and/or dephosphorylation by PP2A yields a mixture of phosphorylated forms which cannot be separated, especially not the two monophospho forms. Therefore, using site-directed mutagenesis, each phosphorylation site is eliminated separately by exchanging serine against alanine (cTnI-S22A, cTnI-S23A). These mutated proteins are overexpressed in *E. coli* and purified to homogeneity (see Materials and Methods). Corresponding mono- and bisphosphorylated cTnI forms are obtained by phosphorylation with PKA. In parallel, pseudo-mono- and pseudo-bisphosphorylated cTnI forms are generated by replacing each serine residue against aspartate. These proteins are referred to as cTnI-S22D, cTnI-S23D, and cTnI-S22D-S23D. They are as well overexpressed in *E. coli*. Purification to homogeneity includes chromatography on CM-Sepharose and on an affinity matrix, cTnC−Sepharose. Homogeneity and correctness of the isolated proteins are checked by SDS gel electrophoresis, N-terminal sequence analysis, and mass spectrometry (data not shown).

Table 1: Nomenclature and Phosphate Content of Employed Recombinant cTnI Forms[a]

cTnI form	mol of P/mol of cTnI	phospho form	dephospho form
cTnI-WT	1.8 ± 0.2	cTnI-WT-bP	cTnI-WT-dP
cTnI-S22A	1.0 ± 0.1	cTnI-S22A-mP	cTnI-S22A-dP
cTnI-S23A	0.9 ± 0.15	cTnI-S23A-mP	cTnI-S23A-dP

[a] Means of the phosphorylation degree of 4 different preparations of each of the recombinant cTnI forms are given with standard deviations. Isolation and phosphorylation by PKA are performed as described under Materials and Methods.

These isolated and mutated cTnI proteins are employed as substrates for PKA. Table 1 shows that cTnI-WT can be phosphorylated to a degree of 2 mol of phosphate incorporated/mol of protein at the two serine residues, serine 22 and serine 23. cTnI-S22A and cTnI-S23A are phosphorylated to a degree of 1 mol of phosphate incorporated/mol of protein as expected (Table 1). These proteins are employed in the SPR-spectrometry as analytes; the designation of each protein is given in Table 1.

Complex formation of immobilized cTnC with cTnI as analyte is monitored by SPR. In the association phase, increasing concentrations of fully dephosphorylated cTnI-WT in the analyte solution result in an enhanced equilibrium response level (R_{eq}), i.e., the amount of complex formed (Figure 1A). The complex dissociates and releases cTnI when cTnI is omitted from the analyte solution (Figure 1A). Significantly lower equilibrium binding levels are observed when bisphospho-cTnI-WT is used (Figure 1B). The association and dissociation rates of dephospho- and bisphosphorylated cTnI-WT are analyzed; thus, second-order association rate constants as well as first-order dissociation rate constants are determined (Table 2). Employing a set of cTnI concentrations or repetition of a given experiment shows that these constants are reproducible within a standard deviation of 5−10%. Clearly, bisphosphorylation of cTnI reduces the rate of association with cTnC Ca_3 approximately 2-fold (Table 2). In contrast, the rate of dissociation does not change. Indeed, as will be shown below, the dissociation rate constants of all cTnI/cTnC Ca_3 complexes are identical within standard error of the mean. As a consequence, bisphosphorylation reduces the affinity of cTnI to cTnC Ca_3 nearly 2-fold independently of the dephospho form employed, WT, S22A, or S23A (Table 2).

All three of these dephospho cTnI forms dissociate from cTnC Mg_2 approximately 5-fold faster than from cTnC Ca_3 (see Table 2). In contrast, the rate of association is very similar employing Ca^{2+} or Mg^{2+} containing cTnC as ligand. As a result, the affinity of these cTnI forms is 5−6-fold lower to cTnC Mg_2 in comparison to cTnC Ca_3. Bisphosphory-

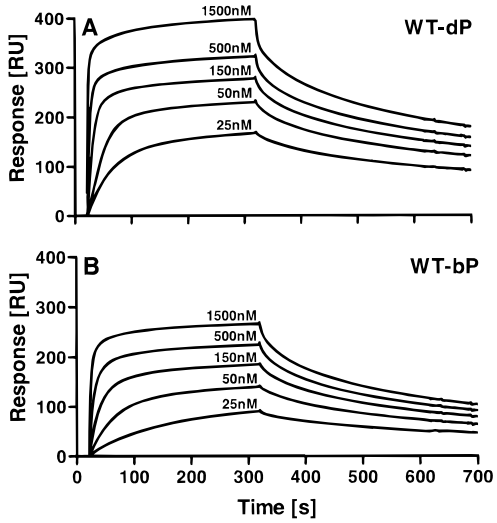

FIGURE 1: Interaction of dephospho- and bisphosphorylated cTnI-WT with immobilized cTnC. 1136 RU of cTnC, labeled with 3 mol of biotin/mol of protein, were immobilized on a streptavidin surface (SA5-chip). cTnI in the range of 25 nM to 1.5 μM was injected for 300 s as indicated. Interaction of cTnI-WT with immobilized cTnC was measured in 20 mM MOPS, 500 mM KCl, 5 mM $MgCl_2$, 0.1 mM $CaCl_2$, 2 mM DTT, pH 8.0 by following the change in the SPR signal (given in RU). (A) cTnI-WT-dP and (B) cTnI-WT-bP were employed as analytes. Dissociation was recorded in the same buffer without cTnI being present.

lation of cTnI-WT again decreases the association rate with cTnC Mg_2 ca. 1.6-fold and increases additionally the dissociation rate also ca. 1.7-fold. Thus, the affinity is reduced about 3-fold.

Figure 2A,B shows the effect of the two consecutive phosphorylation steps on the cTnC−cTnI interaction. The dephosphorylated cTnI forms are compared with the corresponding mono- and bisphosphorylated forms at one fixed cTnI concentration. Monophosphorylation at either site, serine 22 or serine 23, reduces the equilibrium binding level by ca. 20%; bisphosphorylation exerts about twice the effect. This effect is seen similarly with cTnC Mg_2 or cTnC Ca_3 as ligand (compare Figure 2A and Figure 2B).

Under identical experimental conditions, a set of cTnI concentrations was tested as shown exemplarily in Figure 1. Fitting these curves allows calculation of the association and dissociation rate constants as well as affinity constants (Table 2). Most clearly, the dissociation rate constants of all complexes formed with cTnC Ca_3 are identical within the standard error of the mean; i.e., dissociation of the formed cTnI/cTnC complexes is independent of the phosphorylation state of cTnI (Table 2). Significant differences in the rate of association with cTnC Ca_3 are seen by comparing dephospho- with monophosphorylated and bisphosphorylated cTnI. (Rate constants are defined different if a p-value < 0.05 is calculated in the t-test analysis; see Materials and Methods.) It should be pointed out that the mean values for the dissociation rate constants are calculated from 27 independent measurements and that reproducibility of each value is extremely high as expressed by a very low standard error of 2.3%. The standard deviation of each association rate constant determined separately is always below 10% (for details, see Table 2).

Monophosphorylation at either site, serine 22 or serine 23, reduces the association rate constant approximately 1.5-fold and bisphosphorylation about 1.9-fold. Thus, the affinity of cTnI is reduced stepwise first by monophosphorylation at serine 22 or serine 23 and then by bisphosphorylation. A similar, however smaller, stepwise reduction in the association rate constants by mono- (1.2-fold) and bisphosphorylation (1.6-fold) is seen with cTnC Mg_2 (Table 2). The three phospho forms of cTnI dissociate from cTnC Mg_2 with different rates, in contrast to the identical dissociation rates of these forms from cTnC Ca_3 (Table 2). Thus, bisphosphorylation enhances this rate more than monophosphorylation does, and the monophosphorylated forms again show a higher rate of dissociation than the dephosphorylated forms (Table 2). There is also a significant difference in the dissociation rate between the two mutant forms, S22A and S23A. Overall, the affinity of cTnI to cTnC Mg_2 decreases from 2.5×10^7 to 1.4×10^7 and finally to 0.9×10^7 M^{-1} by comparing the dephospho- with the mono- and bisphosphorylated forms (Table 2).

Similar stepwise changes are obtained by exchanging serine 22 or serine 23 or both serine residues against aspartate. Again the equilibrium binding level of the monoaspartate derivatives is reduced to a lesser extent than that of the bisaspartate derivative (Figure 2C). There is no significant difference if a negative charge, i.e., one aspartate residue, is present at position 22 or 23. Again, the dissociation rates of all cTnI proteins from cTnC Ca_3 including the three aspartate-containing forms are identical within the standard error of the mean (Figure 3 and Table 2). In contrast, the rate of association with cTnC Ca_3 decreases ca. 1.4-fold and 1.7-fold comparing the monoaspartate- and bisaspartate-containing cTnI forms with the cTnI-WT form. No significant difference exists between the two monoaspartate derivatives, and also their association rate constants are intermediate and between that of cTnI-WT and that of the bisaspartate form (Table 2). Similar to what has been observed employing different cTnI phospho forms, more subtle differences in the rate of dissociation are apparent employing Mg^{2+}- instead of Ca^{2+}-saturated cTnC as ligand. As in the case of the phospho-cTnI forms, the bisaspartate derivative shows an enhanced rate of dissociation (ca. 1.5-fold) in comparison to the dephospho-cTnI-WT. However, the monoaspartate derivatives do not differ significantly from the bisaspartate derivative (Table 2).

Complex formation of dephosphorylated cTnT purified from bovine hearts with cTnI can be seen by immobilizing cTnT on the sensor chip and employing cTnI as analyte. Figure 3 shows that at all cTnI concentrations employed the equilibrium binding level of the bisphosphorylated cTnI form is lower than that of the dephosphorylated form. The rate of association of cTnI with cTnT is approximately 1000-fold slower than the rate of association of cTnI with cTnC (Table 3). The rate of dissociation is approximately in the same order of magnitude (compare Table 2 and Table 3). As in the case of the dephospho, monophospho, and bisphospho cTnI forms, the rate of dissociation of these cTnT/cTnI complexes is identical within the standard error of the mean. All phospho derivatives, monophospho or bisphospho cTnI, show a reduced rate of association in comparison to the dephosphorylated forms; furthermore, the association rate constants do not differ between mono- or bisphosphorylated cTnI forms (Table 3). Accordingly, the

Table 2: Rate and Affinity Constants for the Interaction of Phospho and Dephospho Forms of Different cTnI Forms with Immobilized cTnC[a]

	cTnC Ca_3[b]			cTnC Mg_2[b]		
cTnI form	$k_a \times 10^{-5}$ (s^{-1} M^{-1})	$k_d \times 10^2$ (s^{-1})	$K_A \times 10^{-7}$ (M^{-1})	$k_a \times 10^{-5}$ (s^{-1} M^{-1})	$k_d \times 10^2$ (s^{-1})	$K_A \times 10^{-7}$ (M^{-1})
cTnI-WT-d	P6.1 ± 0.3		15.0 ± 0.8	5.0 ± 0.3	2.0 ± 0.2	2.5 ± 0.3
cTnI-S23A-dP	6.1 ± 0.2		15.0 ± 0.6	4.8 ± 0.4	2.1 ± 0.1	2.5 ± 0.3
cTnI-S22A-dP	5.5 ± 0.3		13.0 ± 0.8	4.5 ± 0.4	1.8 ± 0.2[c]	2.5 ± 0.2
cTnI-S23A-mP	4.1 ± 0.3[a]		9.8 ± 0.8	4.0 ± 0.3[b]	2.8 ± 0.2[c]	1.4 ± 0.1
cTnI-S22A-mP	3.7 ± 0.3[a]	0.42 ± 0.01	8.8 ± 0.7	3.8 ± 0.2[b]	2.7 ± 0.1[d]	1.4 ± 0.1
cTnI-WT-bP	3.2 ± 0.3[a]		7.6 ± 0.7	3.1 ± 0.3[b]	3.4 ± 0.1[d]	0.9 ± 0.1
cTnI-S22D	4.2 ± 0.3[a]		10.0 ± 0.8	4.1 ± 0.3[b]	2.5 ± 0.2[d]	1.6 ± 0.2
cTnI-S23D	4.3 ± 0.4[a]		10.0 ± 1.0	4.4 ± 0.4[b]	2.8 ± 0.2[d]	1.6 ± 0.2
cTnI-S22D−S23D	3.5 ± 0.3[a]		8.3 ± 0.7	3.5 ± 0.2[b]	2.8 ± 0.2[d]	1.3 ± 0.1

[a] Association rate constants (k_a) for the interaction of cTnI with cTnC Ca_3 are calculated employing the first 100 s after injection of the analyte (Figures 2 and 3). The association phase of the interaction with cTnC Mg_2 is evaluated for the first 60 s according to eq 11 (see Materials and Methods). Dissociation rate constants (k_d) are calculated 6 s after finishing injection of cTnI over a range of 60 s using eq 13. Mean k_a values are shown with standard deviations ($n = 4$ preparations) for de-, mono-, and bisphosphorylated cTnI forms and ($n = 3$ preparations) for all Asp mutants. k_d values of all cTnI forms are determined separately as well. The obtained k_d values for the interaction of cTnI with cTnC Ca_3 are statistically not significantly different ($p > 0.05$; determined as described under Materials and Methods). Therefore, one mean value is calculated with a standard error of the mean. The superscripts a and b define k_a values significantly different ($p < 0.05$) from those of cTnI-WT-dP to cTnCCa_3 and cTnCMg_2, respectively. Superscript c defines k_d values significantly different ($p < 0.05$) for the two mutant proteins S22A and S23A from cTnCMg_2. Superscript d defines k_d values significantly different ($p < 0.05$) from that of cTnI-WT-dP employing cTnCMg_2 as a ligand. [b] The stoichiometry of cTnC−metal complexes is designated as described by (*26*).

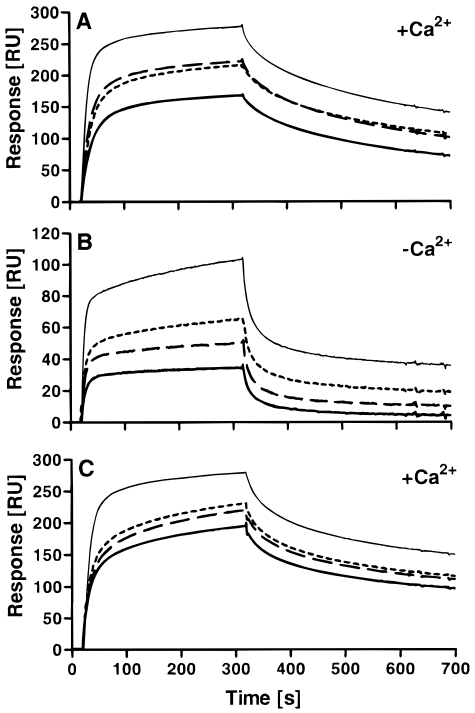

FIGURE 2: Interaction of dephospho-, mono-, and bisphosphorylated cTnI with immobilized cTnC. Interaction studies between cTnI to the immobilized cTnC Ca_3 were performed as described in Figure 1. As analytes (150 nM each), the following were employed: cTnI-WT-dP (thin solid line); cTnI-S23A-mP (- - -); cTnI-S22A-mP (− −); and cTnI-WT-bP (thick solid line) to (A) cTnC Ca_3 or to (B) cTnC Mg_2 (0.1 mM $CaCl_2$ replaced by 2 mM EGTA). In (C) the following cTnI forms at 150 nM were employed: cTnI-WT-dP (thin solid line); cTnI-S22D (- - -), cTnI-S23D (− −); and cTnI-S22D−S23D (thick solid line). For calculation of rate constants, four different concentrations were used (not shown).

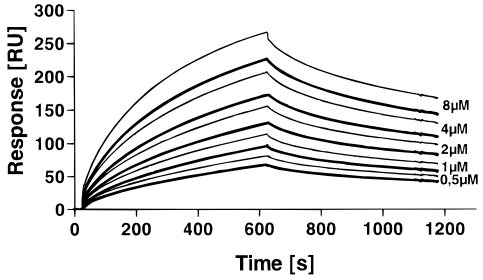

FIGURE 3: Interaction of dephospho- and bisphosphorylated cTnI-WT with immobilized cTnT. 780 RU of cTnT labeled with 3 mol of biotin/mol of protein were immobilized on a SA5-chip. cTnI in the range of 0.5−8 μM was injected for 600 s as indicated. The interaction of cTnI with cTnT was studied in 20 mM MOPS, 500 mM KCl, 5 mM $MgCl_2$, 2 mM DTT, pH 8.0, and dissociation was measured in the same buffer without cTnI. The plot shows the interaction of cTnI-WT-dP (thin line) and cTnI-WT-bP (thick line) with cTnT using concentrations as indicated on the plot.

affinity of all cTnI phospho derivatives is nearly identical and lower than that of the dephospho forms (Table 3).

Whereas a difference in the association rate constants of cTnT with the phospho and dephospho cTnI forms can be observed (see above), these differences disappear when the cTnC Ca_3/cTnI complexes react with immobilized cTnT (Table 4). The association rate constants of all these complexes are statistically not significantly different; therefore, only one mean value is given (Table 4). However, a reduction in the equilibrium binding level is seen when

Table 3: Rate and Affinity Constants for the Interaction of cTnI with Immobilized cTnT[a]

cTnI forms	$k_a \times 10^{-2}$ (s^{-1} M^{-1})	$k_d \times 10^2$ (s^{-1})	$K_A \times 10^{-5}$ (M^{-1})
cTnI-WT-dP	4.7 ± 0.4		4.4 ± 0.4
cTnI-S23A-dP	4.1 ± 0.4		3.8 ± 0.4
cTnI-S22A-dP	4.4 ± 0.3	10.7 ± 0.2	4.1 ± 0.3
cTnI-S23A-mP	3.4 ± 0.3*		3.2 ± 0.3
cTnI-S22A-mP	3.7 ± 0.3*		3.5 ± 0.3
cTnI-WT-bP	3.9 ± 0.3*		3.6 ± 0.3

[a] Association rate constants (k_a) were determined for 300 s starting with the injection employing eq 11 (see Materials and Methods). Dissociation rate constants (k_d) were determined 6 s after finishing injection and over the range of 200 s (Figure 4) using eq 13. Mean k_a values are shown with standard deviations ($n = 3$ preparations) for dephospho-, mono-, and bisphosphorylated cTnI forms. k_d values of all cTnI forms were determined separately. Since the obtained k_d values were statistically not significantly different ($p > 0.05$; determined as described in Table 2), only one mean value was calculated with a standard error of the mean. The superscript asterisk defines k_a values significantly different ($p < 0.05$) from that of cTnI-WT-dP employing cTnT as a ligand.

Table 4: Rate and Affinity Constants for the Interaction of Different cTnI/cTnC Ca_3 Complexes with Immobilized cTnT[a]

cTnI/cTnC complexes	$k_a \times 10^{-2}$ (s^{-1} M^{-1})	$k_d \times 10^5$ (s^{-1})	$K_A \times 10^{-6}$ (M^{-1})
cTn Ca_3/cTnI-WT-dP		7.3 ± 0.5	6.2 ± 0.4
cTn Ca_3/cTnI-S23A-dP		7.4 ± 0.7	6.1 ± 0.6
cTn Ca_3/cTnI-S22A-dP	4.5 ± 0.1	7.0 ± 0.5	6.4 ± 0.5
cTn Ca_3/cTnI-S23A-mP		9.2 ± 0.8	4.9 ± 0.4
cTn Ca_3/cTnI-S22A-mP		8.8 ± 0.7	5.1 ± 0.4
cTn Ca_3/cTnI-WT-bP		9.9 ± 0.8*	4.5 ± 0.4

Association rate constants (k_a) were determined as described in Table 3. Dissociation rate constants (k_d) were determined using eq 13 over a range of 300 s (Figure 5). Mean k_d values with standard deviations ($n = 7$ preparations) for dephospho-, mono-, and bisphosphorylated cTnI forms were calculated. k_a values of all cTnI forms were determined separately ($n = 3$ preparations). The obtained k_a values were statistically not significantly different ($p > 0.05$; determined as described in Table 2). Therefore, one mean value was calculated with a standard error of the mean. Measurements were performed in 20 mM MOPS, 500 mM KCl, 5 mM $MgCl_2$, 0.1 mM $CaCl_2$, 2 mM DTT, pH 8.0. The superscript asterisk defines k_d values significantly different ($p < 0.05$) from that of cTnI-WT-dP employing cTnT as a ligand.

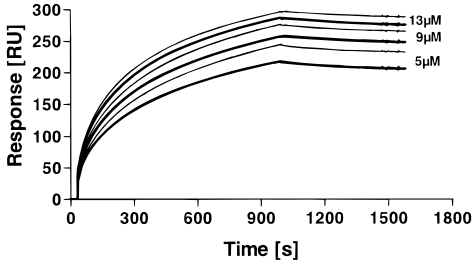

FIGURE 4: Interaction of the dephospho- and monophosphorylated forms of cTnI-S22A containing cTnC/cTnI complex with immobilized cTnT. cTnC/cTnI complexes containing cTnI-S22A-dP (thin line) and cTnI-S22A-mP (thick line) were injected on a cTnT surface (see Figure 4) using concentrations between 5 and 13 μM as indicated on the plot. Dissociation was initiated 16 min after injection of the analyte by omitting the cTnC/cTnI complexes from the buffer.

monophosphorylated cTnI complexed to cTnC Ca_3 binds to cTnT instead of a complex containing the dephosphorylated cTnI (Figure 4). In this instance, the difference in affinity is due to a change in the dissociation rate constant (Table 4). There is no significant difference in the dissociation rate constants between all dephosphorylated cTnI forms; they are higher, however, for all phosphorylated forms. Accordingly, the affinity of all complexes containing dephosphorylated cTnI is higher than those containing either mono- or bisphosphorylated cTnI forms (Table 4).

Independently, the affinity of cTnT to the cTnI/cTnC Ca_3 complex can be determined by analytical gel filtration. The half-lifetime of the dephospho- cTnI-WT-containing cTn holo complex is ca. 2.7 h (calculated from data in Table 4). Thus, analytical gel filtration requiring 15−20 min is fast in comparison to this half-time. After an equilibrium time of ca. 5 times the half-lifetime, gel filtration allows us to determine which subunits dissociate from the cTn holo complex. For that purpose, the cTn holo complex is reconstituted with FITC-labeled cTnC, allowing fluorometric detection of all cTnC-containing complexes. At high protein concentrations during preequilibration ($>10^{-5}$ M), the holo complex elutes as one symmetrical peak with a retention time of 16.4 ± 0.04 min ($n = 5$) (Figure 5 inset). Dissociation is induced by dilution. At a 10 times lower protein

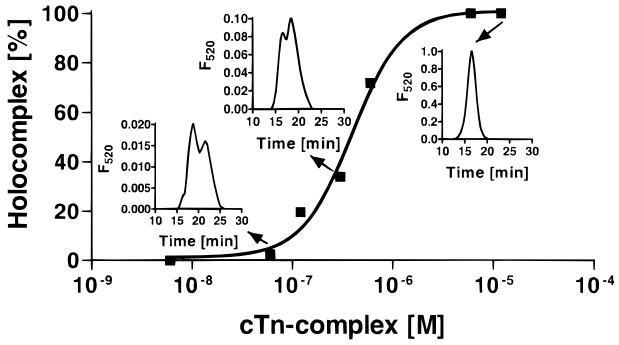

FIGURE 5: Determination of the apparent dissociation constant of the reconstituted cTn complex. Analytical gel filtration was performed in 20 mM MOPS, 500 mM KCl, 5 mM $MgCl_2$, 0.1 mM $CaCl_2$, 2 mM DTT, pH 8.0. Varying concentrations (12, 6, 0.6, 0.3, and 0.12 μM; 60 and 6 nM) of cTn holo complex, reconstituted with dephosphorylated cTnT, cTnI-WT-dP, and FITC-labeled cTnC were injected on a Superdex 200 PC (3.2/30) column. The elution of cTn, of cTnC/cTnI complex, and of cTnC was detected by an on-line fluorometer (excitation wavelength, 495 nm; emission wavelength, 520 nm) as shown in the inserts. The percentage of cTn complex was calculated from the peak area of the fluorescence labeled protein complexes after base line correction.

concentration ($\sim 10^{-6}$ M), additionally the cTnI/cTnC complex, eluting at 18.7 ± 0.13 min ($n = 3$), is observed, and at a protein concentration of $\sim 10^{-8}$ M, the cTnI/cTnC complex and additionally free cTnC, eluting at 21.5 ± 0.15 min ($n = 5$), can be seen (Figure 5 insets). From the peak areas, the amount of remaining cTn holo complex can be calculated at each protein concentration in the preequilibrium mixture. A plot of the amount of cTn holo complex versus protein concentration yields a K'_A of 0.3×10^7 M^{-1}.

Up to this point, mono- or bisphosphorylation of cTnI revealed differences in the rate of association with either cTnC or cTnT and also in the rate of dissociation of the cTn holo complex. Therefore, it is interesting to see if this effect of phosphorylation is propagated to the interaction of the ternary cTn holo complex with tropomyosin. For that purpose, ternary cTn holo complexes were reconstituted employing completely dephosphorylated, each monophosphorylated, or bisphosphorylated cTnI. The rate of association as well as that of dissociation of these holocomplexes with tropomyosin is very fast, indeed too fast for determination of rate constants in the Biacore instrument (not shown). Affinity constants, however, can be calculated by plotting the equilibrium binding level as a function of the holo complex concentrations. Scatchard plot analysis yields a K'_A of about 1.45×10^7 M^{-1} for all complexes containing dephosphorylated cTnI forms. There seems to be a slight decrease to 1.39×10^7 M^{-1} employing the monophospho cTnI form and again a slight decrease to 1.29×10^7 M^{-1} employing the bisphospho-cTnI-containing complex. However, these differences are within the estimated standard errors (not shown).

DISCUSSION

Surface plasmon resonance allows a direct observation of the association and dissociation rates separately. Thereby, minute differences in the equilibrium binding behavior of the cTn subunits due to phosphorylation of cTnI can be attributed to changes in these rate constants. All measure-

ments display an extremely high accuracy with a standard error within the same experiment of less than 1%. Repetition of one experiment with one and the same protein form or with different preparations of one protein yields standard deviations of less than 10%. Although errors due to machine parameters are low, systematic errors have to be considered. A principle problem exists in the steric hindrance which is created by the immobilization of the ligand via primary amines to the dextran surface of a sensor chip. For instance, only when cTnC is immobilized, differences in the association with the different cTnI phospho forms are detected; vice versa, the association of cTnC with immobilized cTnI does not reveal these differences (data not shown). Immobilization of cTnI on multiple surface points may suppress intramolecular movements and thus mask conformational differences existent in the different cTnI phospho forms. Further errors might occur due to mass-transfer-limited reactions during the interaction. Control experiments, however, e.g., increasing the flow rates 10-fold or employing lower immobilization levels, did not change the rate constants. Rebinding was excluded by adding nonimmobilized ligand simultaneously with the buffer in the dissociation phase using the same concentration as the immobilized ligand. Again no difference in the dissociation rate constant was detected (data not shown). Multiple complex formation is difficult to access with SPR since this method only detects changes in mass. However, the binding stoichiometry of analyte to ligand was 0.7 and 0.4 for cTnI/cTnC and for holo complex formation, respectively, making formation of polymer complexes unlikely (data not shown). These principle problems seem not to be of major importance, since interaction of the cTn subunits in solution, as determined by gel filtration, results in almost identical affinity constants as determined with immobilized cTn subunits by SPR. The affinity constant of 0.3×10^7 M^{-1}, determined by analytical gel filtration [for a detailed description of the method, see (*23*)], is in good agreement with the value of 0.6×10^7 M^{-1} determined using SPR.

Previous studies, employing fluorescently labeled cTnC, have demonstrated that bisphosphorylation of native bovine cTnI (*26*) or of mutated cTnI forms (*28*) reduces the affinity to cTnC. The degree in reduction is within a factor of ca. 2 identical to what has been determined here by SPR spectroscopy. In none of these studies were monophosphorylated cTnI forms employed. Here, for the first time, it is shown that monophosphorylation influences the interaction of cTnI with cTnC. The SPR studies reveal clearly that the affinity of cTnC for both monophospho-cTnI forms is lower than that for wild-type dephospho-cTnI and that bisphospho-cTnI exhibits a lower affinity to cTnC Ca_3 than each monophospho form. These differences are small; however, they are statistically highly significant. Furthermore, the binding curves of the monophospho forms, as monitored in the Biacore instrument, are observed reproducibly between those of the dephospho and the bisphospho forms (compare Figure 2), corroborating these small differences. In addition, the same stepwise reduction in affinity is observed with cTnI containing one aspartate either at position 22 or at position 23 up to the form containing two aspartate residues.

Liao et al. (*26*) have concluded previously that bisphosphorylation causes a collapse of cTnI from an asymmetrical form to a more symmetrical shape which was correlated with the reduction in affinity to cTnC. The data presented here indicate that a conformational change occurs upon monophosphorylation of cTnI; i.e., phosphorylation may change an equilibrium between two conformations, and bisphosphorylation changes this equilibrium to a higher degree than monophosphorylation does.

Once a cTnC Ca_3/cTnI complex is formed, mono- or bisphosphorylation of the cTnI N-terminus does not seem to influence anymore the conformation of these formed complexes, or in other words, these differences in the conformation of free cTnI are covered by the strong interaction with cTnC Ca_3. This can be concluded from three observations:

First, the dissociation of mono- or bisphosphorylated cTnI from cTnC Ca_3 complexes as well as both monoaspartate- or bisaspartate-substituted cTnI forms from cTnC Ca_3 is identical within the standard error of the mean.

Second, mono- or bisphosphorylation seems to influence the reaction of cTnI with cTnT in a fashion similar to what is observed with cTnC (compare Tables 2 and 3). Again phosphorylation reduces the rate of association; however, once the cTnT/cTnI complex has been formed, no difference is observed in the rate of dissociation. Thus, the complex formation with cTnT results in the disappearance of the differences in the conformation of free cTnI.

Third, there seems hardly to be a difference in the rate of association of the cTnC Ca_3/cTnI complexes—containing either de-, mono-, or bisphosphorylated cTnI—with cTnT; i.e., these formed cTnI/cTnC complexes all seem to have an identical conformation. Thus, this equalization of the cTnI conformations seems to be due to the very tight interaction with cTnC Ca_3 or with cTnT.

Different conformations of cTnI according to the state of phosphorylation can be adopted only in weaker complexes such as with cTnC Mg_2. The interaction of cTnI with cTnC Mg_2 is 6−8-fold weaker than with cTnC Ca_3 (see Table 2), which seems to allow different cTnI conformations within the binary complex reflected in the different dissociation rate constants of these complexes. A similar effect is observed when cTnT forms the ternary complex with cTnI/cTnC Ca_3; again, the dissociation rates differ with mono- and bisphosphorylated cTnI.

These three sets of experiments indicate that different conformational states of cTnI are induced by either mono- or bisphosphorylation. ^{31}P NMR studies have shown that only the bisphospho form of cTnI interacts with another subunit of the cTn holo complex; the monophospho forms do not reveal such an interaction (*17*). Furthermore, these studies show also that the phospho groups in both monophospho-cTnI forms do not interact with the core of cTnI itself.

It is, therefore, not easy to understand how phosphorylation at either site, serine 22 or serine 23, or bisphosphorylation could induce a conformational change in cTnI if these phosphate groups do not interact with other amino acid side chains of cTnI. A solution for this problem could be that the N-terminal extension of cTnI stabilizes the elongated form by interacting only in the nonphosphorylated form with the core of cTnI. This interaction would then be inhibited by stepwise increasing the degree of phosphorylation, i.e., by monophosphorylation of serine 22 or 23 and bisphosphorylation. Thus, an equilibrium between the elongated and

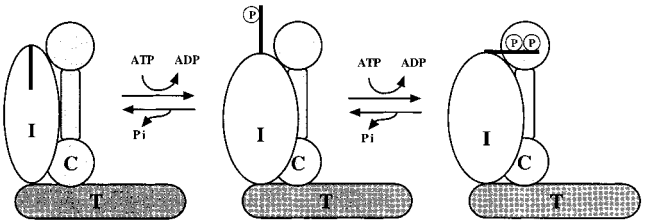

FIGURE 6: Modulation of troponin subunit interaction in response to phosphorylation. Monophosphorylation (P) at the heart-specific N-terminal extension (boldface line) of cTnI (I) causes a dislocation of this N-terminal extension from the core of cTnI, allowing a conformational change by switching from an elongated to a more symmetrical form. Addition of the second phosphate group induces an additional interaction with cTnC (C). Both mono- and bisphosphorylation of cTnI cause a gradual decrease in the affinity between cTnI and cTnC as well as cTnT (T). This effect is reversed by dephosphorylation, releasing inorganic phosphate (Pi).

the more symmetrical shape of cTnI would be gradually shifted to the more symmetrical shape by mono- and consecutively by bisphosphorylation of cTnI. Such a model would not require a direct interaction of the phosphate groups with the core of cTnI, which is in agreement with our ^{31}P NMR data. This situation is opposite to what can be observed in glycogen phosphorylase. Here phosphorylation of serine 14 leads to an ionic interaction of the phosphate group with two arginine residues (Arg 61 and 74), and an equilibrium between a noninteracting and interacting conformation can be seen in the ^{31}P NMR spectrum (*29*).

As mentioned above, ^{31}P NMR data show that holo complex formation puts the two phosphate groups of the bisphosphorylated cTnI form in a different chemical environment from each monophospho form (*17*). Influences on the conformation of skeletal muscle TnI by holo complex formation with skeletal muscle TnT and TnC have been described by Luo et al. (*30*). Only holo complex formation, i.e., the interaction of the sTnC/sTnI complex with sTnT, leads to an elongation of sTnI by ~10 Å (*30*). Due to the high sequence similarity between cardiac and skeletal muscle TnI in the core of the molecule, one could assume that a similar conformational change is induced in cTnI by holo complex formation, too, which allows the interaction of the two phosphates in the bisphospho form with either cTnC or cTnT.

A model showing the effect of cTnI phosphorylation on the holotroponin complex can be formulated (Figure 6).

The dephosphorylated heart specific N-terminal extension of cTnI probably interacts with the core of cTnI to produce the asymmetrical form. An indication for the reaction of the N-terminal extension with the core is the small difference in the dissociation rate between cTnT-S22A and -S23A from cTnC Mg_2. The dephosphorylated N-terminal extension may stabilize the more asymmetric shape of cTnI as discussed above. Mono- or bisphosphorylation would inhibit this interaction which allows a transition to the more symmetrical form. As a consecutive step, only bisphosphorylation would lead to an interaction of the N-terminal extension with cTnC which would cause the reduction in Ca^{2+} affinity.

There is only a very minor influence of these different conformational states of cTnI present in the holo complex on the interaction with tropomyosin. Effects seen are in the same direction as seen in the holotroponin complexes; however, they are statistically not significant. The existence of different conformational states of the cTn complex implies that there might be a physiological function correlated with these states. It is amply documented that formation of the bisphosphorylated state causes a reduction in the affinity of cTnC for Ca^{2+} (*14*, *16*, *31*). In contrast monophosphorylation of cTnI does not seem to have an influence on the Ca^{2+} affinity of cTnC (*13*). However, monophosphorylation of cTnI seems to correlate with an increase in the force of contraction in cardiac muscle (*4*). Therefore, it is plausible to conclude that the conformational transition caused by monophosphorylation of cTnI is responsible for this increase in force. What could be the molecular mechanism remains, however, unclear and therefore is the major question in this area to be solved in the future.

ACKNOWLEDGMENT

We thank G. Gregor for expert secretarial work and B. Kachholz and P. Goldmann for excellent technical assistance.

REFERENCES

1. Farah, C. S., and Reinach, F. C. (1995) *FASEB J. 9*, 755−767.
2. Solaro, R. J. (1995) *Adv. Exp. Med. Biol. 382*, 109−115.
3. England, P. J. (1975) *FEBS Lett. 50*, 57−60.
4. England, P. J. (1976) *Biochem. J. 160*, 295−304.
5. Solaro, R. J., Moir, A. J., and Perry, S. V. (1976) *Nature 262*, 615−617.
6. Mittmann, K., Jaquet, K., and Heilmeyer, L. M., Jr. (1990) *FEBS Lett. 273*, 41−45.
7. Swiderek, K., Jaquet, K., Meyer, H. E., Schächtele, C., Hofmann, F., and Heilmeyer, L. M., Jr. (1990) *Eur. J. Biochem. 190*, 575−582.
8. Vallins, W. J., Brand, N. J., Dabhade, N., Butler-Browne, G., Yacoub, M. H., and Barton, P. J. (1990) *FEBS Lett. 270*, 57−61.
9. Murphy, A. M., Jones, L., Sims, H. F., and Strauss, A. W. (1991) *Biochemistry 30*, 707−712.
10. Mittmann, K., Jaquet, K., and Heilmeyer, L. M., Jr. (1992) *FEBS Lett. 302*, 133−137.
11. Jaquet, K., Thieleczek, R., and Heilmeyer, L. M., Jr. (1995) *Eur. J. Biochem. 231*, 486−490.
12. Ardelt, P., Dorka, P., Jaquet, K., Heilmeyer, L. M., Jr., Kortke, H., Korfer, R., and Notohamiprodjo, G. (1998) *J. Biol. Chem. 379*, 341−347.
13. Zhang, R., Zhao, J., and Potter, J. D. (1995) *J. Biol. Chem. 270*, 30773−30780.
14. Zhang, R., Zhao, J., Mandveno, A., and Potter, J. D. (1995) *Circ. Res. 76*, 1028−1035.
15. Wattanapermpool, J., Guo, X., and Solaro, R. J. (1995) *J. Mol. Cell. Cardiol. 27*, 1383−1391.
16. Reiffert, S. U., Jaquet, K., Heilmeyer, L. M., Jr., Ritchie, M. D., and Geeves, M. A. (1996) *FEBS Lett. 384*, 43−47.
17. Jaquet, K., Korte, K., Schnackerz, K., Vyska, K., and Heilmeyer, L. M., Jr. (1993) *Biochemistry 32*, 13873−13878.
18. Al-Hillawi, E., Minchin, S. D., and Trayer, I. P. (1994) *Eur. J. Biochem. 225*, 1195−1201.
19. Gahlmann, R., Wade, R., Gunning, P., and Kedes, L. (1988) *J. Mol. Biol. 210*, 379−391.
20. Babu, A., Su, H., Ryu, Y., and Gulati, J. (1992) *J. Biol. Chem. 267*, 15469−15474.
21. Villar-Palasi, C., and Kumon, A. (1981) *J. Biol. Chem. 256*, 7409−7415.
22. Perry, S. V., and Cole, H. A. (1974) *Biochem. J. 141*, 733−743.
23. Herberg, F. W., and Taylor, S. S. (1993) *Biochemistry 32*, 14015−14022.
24. Szabo, A., Stolz, L., and Granzow, R. (1995) *Curr. Opin. Struct. Biol. 5*, 699−705.
25. Stenberg, E., Persson, B., Roos, H., and Urbaniczky, C. (1991) *J. Colloid Interface Sci. 143*, 513−526.

26. Liao, R., Wang, C. K., and Cheung, H. C. (1994) *Biochemistry 33*, 12729−12734.
27. Karlsson, R., and Falt, A. (1997) *J. Immunol. Methods 200*, 121−133.
28. Dong, W. J., Chandra, M., Xing, J., Solaro, R. J., and Cheung, H. C. (1997) *Biochemistry 36*, 6745−6753.
29. Sperling, J. E., Feldmann, K., Meyer, H., Jahnke, U., and Heilmeyer, L. M., Jr. (1979) *Eur. J. Biochem. 101*, 581−592.
30. Luo, Y., Wu, J. L., Gergely, J., and Tao, T. (1997) *Biochemistry 36*, 11027−11035.
31. Robertson, S. P., Johnson, J. D., Holroyde, M. J., Kranias, E. G., Potter, J. D., and Solaro, R. J. (1982) *J. Biol. Chem. 257*, 260−263.

BI980280J